The Biotin Repressor: Thermodynamic Coupling of Corepressor Binding, Protein Assembly, and Sequence-Specific DNA Binding†

Emily D. Streaker, Aditi Gupta, and Dorothy Beckett*

Department of Chemistry and Biochemistry, College of Life Sciences, University of Maryland, College Park, Maryland 20742

Received May 24, 2002

ABSTRACT: The *Escherichia coli* biotin repressor, an allosteric transcriptional regulator, is activated for binding to the biotin operator by the small molecule biotinyl-5′-AMP. Results of combined thermodynamic, kinetic, and structural studies of the protein have revealed that corepressor binding results in disorder to order transitions in the protein monomer that facilitate tighter dimerization. The enhanced stability of the dimer leads to stabilization of the resulting biotin repressor−biotin operator complex. It is not clear, however, that the allosteric response in the system is transmitted solely through the protein−protein interface. In this work, the allosteric mechanism has been quantitatively probed by measuring the biotin operator binding and dimerization properties of three biotin repressor species: the apo or unliganded form, the biotin-bound form, and the holo or bio-5′-AMP-bound form. Comparisons of the pairwise differences in the bioO binding and dimerization energetics for the apo and holo species reveal that the enhanced DNA binding energetics resulting from adenylate binding track closely with the enhanced assembly energetics. However, when the results for repressor pairs that include the biotin-bound species are compared, no such equivalence is observed.

Linked equilibria, which provide a means of controlling the occupancy of transcription regulatory sites by transcription factors, are ubiquitous in the regulation of transcription initiation. Processes that may be coupled to DNA binding by transcription factors include small ligand binding events (*1*), post-translational modification (*2*), and protein−protein interactions (*3*). Furthermore, examples of both positive and negative coupling have been characterized. In the classic allosteric DNA binding systems, including the purine and lac repressors, where the proteins form stable oligomers, binding of a small molecule effector shifts the orientation of the DNA binding domains of the protein monomers, thereby altering the "fit" between the protein and DNA (*4*). In the purine repressor for which the small molecule enhances DNA binding affinity, the fit is improved (*5*), while in the lac repressor in which affinity for DNA is decreased as a consequence of inducer binding, the fit is compromised concomitant with ligand binding (*6*). In an alternative model for allosteric regulation of DNA binding, the allosteric signal dictates the level of occupancy of the transcription regulatory site by altering the assembly energetics of the transcription factor (*7*). This phenomenology is common because, given the oligomeric nature of transcription regulators, the overall stability of the regulatory complex reflects not only the energetics of the protein−DNA interfaces but also the thermodynamic stability of the protein−protein interfaces relevant to these complexes. Assembly of transcription factors can be controlled by post-translational modification, small ligand binding, or other protein−protein interactions (*1*−*3*). However, in systems that function via regulated assembly or disassembly, it is not clear that the functional changes (i.e., occupancy of regulatory sites and thus transcription levels) in the system are solely attributable to changes in the assembly energetics. In short, it is not known if the altered energetics of binding to the DNA regulatory site reflect only altered assembly energetics.

The biotin repressor is an example of a system in which small ligand binding promotes DNA binding by enhancing repressor dimerization (*8*−*10*). The protein serves as the repressor of transcription initiation at the biotin biosynthetic operon (*11*). It is also the enzyme that catalyzes covalent linkage of biotin to the single biotin-dependent carboxylase, acetyl-CoA carboxylase (*11*−*13*). This latter reaction occurs in a two-step process involving the initial synthesis of the adenylate of biotin, biotinyl-5′-AMP, followed by linkage of the biotin to a single lysine residue on the biotin carboxyl carrier protein of the transcarboxylase (*14*). In addition to its function as an enzymatic intermediate, the adenylate promotes binding of BirA to the biotin operator (*15*). BioO binding has been shown to occur by cooperative association of two protein monomers with the two half-sites of the operator (*16*). Furthermore, adenylate binding is positively coupled to BirA dimerization (*8*). Studies of mutants indicate that defects in the ligand binding domain of the protein that result in a decreased level of DNA binding both in vivo and in vitro correlate with a loss of the ability to assemble into dimers (*9*, *12*). The accumulated results suggest an allosteric model in which bio-5′-AMP promotes DNA binding by enhancing the assembly energetics of the protein.

† This work was supported by NIH Grant R01-GM46511 to D.B. The Beckman-Coulter Analytical Ultracentrifuge was purchased with funds obtained through NIH Shared Instrumentation Grant S10-RR15899 to D.B.

* To whom correspondence should be addressed. Phone: (301) 405-1812. Fax: (301) 314-9121. E-mail: db248@umail.umd.edu.

10.1021/bi0203839 CCC: $22.00
Published on Web 11/09/2002

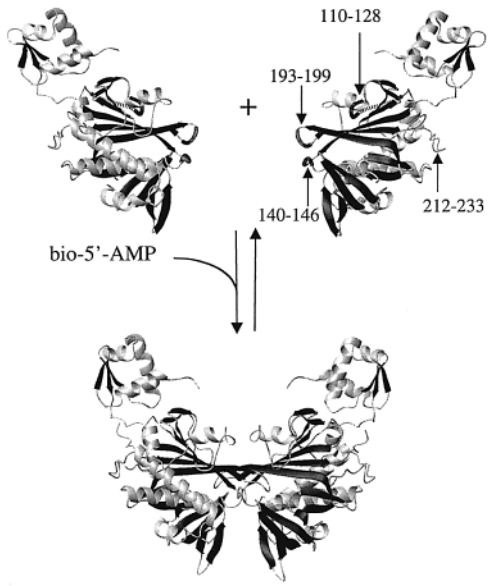

FIGURE 1: Model of allosteric activation of the biotin repressor by ligand binding. Small ligand binding is positively coupled to dimerization of the repressor. The enhanced dimerization energetics result in a more stable protein−DNA complex. The regions of the aporepressor model that appear as springs represent segments of the polypeptide chain that are disordered in the unliganded monomer structure and visible in the structure of the dimer. The locations of the partially disordered loops in the aporepressor are indicated with labels. The models of the aporepressor monomer and the BirA·biotin dimer were created using MolMol (*20*) with Protein Data Bank entries 1BIB and 1HXD, respectively, as input.

Structures of both apoBirA and one liganded form of the protein have been determined by X-ray crystallography (*10*, *17*). The aporepressor is a 35.3 kDa monomer that is folded into three domains: an N-terminal DNA binding domain, a central catalytic domain, and a C-terminal domain that is now known to function in transfer of biotin to the acetyl-CoA carboxylase (*17*−*19*). The aporepressor is also characterized by four partially disordered surface loops that are indicated in Figure 1. The available structure of the BirA dimer is that of the biotin-bound repressor (*10*). Although the substrate biotin is not the physiological corepressor in this system, it has been shown to activate the DNA binding function of BirA, albeit more weakly than does bio-5′-AMP (*15*). In the dimer structure, the interface is formed by side-by-side alignment of the β-sheets of the central domains of each monomer. In addition, three of the four loops that are partially disordered in the aporepressor are located in the dimer interface (Figure 1). While one of these loops was shown by analysis of mutants to participate in biotin, bio-5′-AMP, and bio binding and dimerization, mutations in the other two loops have been shown to perturb only DNA binding and dimerization (*9*, *21*). These combined results have led to the formulation of a model for allostery in this system in which small ligand binding drives folding of these surface loops. The folding stabilizes dimerization by reducing the entropic penalty associated with the process.

To understand linked equilibria, it is important to dissect the quantitative effects on individual interactions and the resulting functional consequences for the system. In a simple transcription control system, the level of occupancy of the DNA regulatory sequences determines function in transcription initiation. In the biotin regulatory system, occupancy of bioO by BirA is regulated by the allosteric effector, bio-5′-AMP, via its influence on assembly energetics. What is not clear is the level of correlation between energetic effects on assembly and bioO binding. In short, does the enhancement in DNA binding affinity associated with bio-5′-AMP binding track with the observed enhancement in dimerization energetics?

This work addresses the quantitative relationship between small ligand binding, dimerization, and DNA binding in the biotin repressor system. The bioO binding properties of three BirA species, apoBirA, BirA·biotin, and BirA·bio-5′-AMP, were determined by DNaseI footprinting. Results of these measurements reveal that all three species bind to the operator specifically and cooperatively. Moreover, while the total Gibbs free energy of bioO binding by BirA·biotin is approximately −1.6 kcal more favorable than that for binding by apoBirA, the physiological effector, bio-5′-AMP, enhances the DNA binding energetics by −4.5 kcal/mol. The assembly properties of the three repressor species were assessed using sedimentation equilibrium. Analysis of these data yields a lower limit for the dimerization constant for apoBirA of 2 mM, a value of approximately 1 mM for the BirA·biotin complex, and a value of 1 μM for holoBirA. The combined results indicate that the difference in assembly energetics for the apoBirA/BirA·bio-5′-AMP pair is equivalent to the difference in bioO binding energetics. However, for any pair of species that includes the biotin-bound protein, no such equivalence is observed.

MATERIALS AND METHODS

Enzymes and Chemicals. The restriction enzymes *Hin*dIII and *Pst*I and the Klenow fragment of DNA polymerase I were obtained from Promega. The DNaseI was purchased from Worthington Biochemicals, and the [α-^{32}P]dATP and dGTP used in the radiolabeling of DNA were from Amersham Pharmacia Biotech. The D-biotin and ATP were from Sigma. All other chemicals used in the preparation of buffers were reagent or analytical grade. Biotinyl-5′-AMP was synthesized in this laboratory and purified as described in ref *14*, and BirA was purified as previously described (*16*).

Preparation of DNA for Footprinting. The plasmid pBioZ (*16*) containing the biotin operator, bioO, was digested with *Hin*dIII, and the resulting 3′-recessed ends were filled in with [α-^{32}P]dATP and dGTP using the Klenow fragment (*22*). Labeled DNA was purified over an Elutip column (Schleicher and Schuell) and then digested with *Pst*I. The resulting restriction fragments were resolved on a 1% agarose gel, and the bioO-containing fragment was recovered by electroelution (*23*). Following purification over an Elutip column, the DNA was concentrated by precipitation, resuspended at a concentration of $\leq$20000 cpm/μL in 10 mM Tris-HCl (pH 8.0) and 0.1 mM EDTA, stored at 4 °C, and used for footprinting for up to 3 weeks.

DNaseI Footprinting. DNaseI footprinting was performed as previously described (*16*) following a modification of the methods outlined by Brenowitz et al. (*22*). The reaction buffer contained 10 mM Tris-HCl (pH 7.5 at 20 °C), 50 mM KCl, 2.5 mM $MgCl_2$, 1 mM $CaCl_2$, 2 μg/mL sonicated calf thymus DNA, and 100 μg/mL BSA. The small ligands biotin or biotin and ATP were present at concentrations at which BirA is known to be saturated with either the substrate or

the intermediate (*24*, *25*). For binding experiments performed in the presence of biotin, the ligand was added to a final concentration of 50 μM. DNA binding experiments performed with biotinyl-5′-AMP included 50 μM biotin and 500 μM ATP. Each 200 μL binding reaction mixture contained 12 000 cpm of radiolabeled DNA at a final concentration of approximately 20 pM and BirA at an appropriate concentration. Reaction mixtures were allowed to equilibrate at 20 °C for 1 h. DNaseI digestion was initiated by the addition of 5 μL of 0.2 μg/mL DNaseI prepared in reaction buffer without calf thymus DNA and BSA immediately prior to use. The digestion was allowed to proceed for 2 min at 20 °C and quenched with 33 μL of 50 mM Na_2EDTA, and the DNA was precipitated by the addition of 700 μL of 0.4 M NH_4OAc and 50 μg/mL tRNA in absolute ethanol. The pellets were washed twice with 500 μL of cold 80% (v/v) absolute ethanol in water and lyophilized. The resulting dried pellets were resuspended in 7 μL of gel loading buffer containing 80% (v/v) deionized formamide, 1× TBE, 0.02% (w/v) bromophenol blue, and 0.02% (w/v) xylene cyanol, heated for 10 min at 90 °C, and separated on a 10% denaturing acrylamide gel.

Sedimentation Equilibrium Measurements. Sedimentation equilibrium was used to determine the assembly properties of the three BirA species. Experiments were carried out using a Beckman Optima XL-I analytical ultracentrifuge equipped with a four-hole An-60 rotor. Either standard 12 or 3 mm double-sectored cells with charcoal-filled Epon centerpieces and saffire windows were used for the experiments. Protein concentration distributions were determined using the absorption optical system of the instrument. All experiments were performed at 20 °C using proteins that had been dialyzed extensively against low-salt standard buffer [10 mM Tris-HCl (pH 7.50 ± 0.02 at 20 °C), 50 mM KCl, and 2.5 mM $MgCl_2$]. Sample volumes were typically 150 μL for the 12 mm cells and 50 μL for the 3 mm cells. The bio-5′-AMP or biotin solutions used in preparing the complexes were themselves prepared by dissolving the appropriate ligand in the dialysate obtained from protein equilibration. In all measurements performed in the presence of ligands, the binding conditions were stoichiometric and the ligand was present at a higher concentration than the protein. Samples were prepared at multiple loading concentrations and centrifuged at multiple rotor speeds (*26*). Scans were acquired as averages of four measurements of absorbance at each radial position, with spacing of 0.002 cm between each radial position. Scans of the biotin repressor bound to bio-5′-AMP were obtained at 295 nm to avoid any contribution from the absorbance of the adenosine moiety of the bio-5′-AMP ligand. Scans of apo-BirA and the complex with biotin were acquired at either 295 or 300 nm, the longer wavelength being utilized for samples prepared at the highest loading concentrations. Extinction coefficients at 295 and 300 nm were calculated on the basis of the known extinction coefficient at 280 nm of 1.3 mM^{-1} cm^{-1} and the ratios of the measured absorbances at 280 nm and the longer wavelengths. The solvent density was determined pycnometrically.

Quantitation and Analysis of Footprints. Footprinting gels were dried, exposed to storage phosphor screens for 40 h, and imaged using a Molecular Dynamics phosphorimaging system (Amersham Pharmacia Biotech). The optical densities of bands representative of each bioO operator half-site at all protein concentrations were integrated and binding curves generated as described by Brenowitz et al. (*22*). All binding data were analyzed by nonlinear least-squares techniques with NonLin (*27*). The low concentration of DNA present in the binding reaction mixtures permits the assumption that the free BirA concentration is equivalent to the total BirA concentration. Data were analyzed using the following equations

$$\bar{Y}_1 = \frac{k_1[\mathrm{P}] + k_1k_2k_{12}[\mathrm{P}]^2}{1 + (k_1 + k_2)[\mathrm{P}] + k_1k_2k_{12}[\mathrm{P}]^2} \quad (1)$$

$$\bar{Y}_2 = \frac{k_2[\mathrm{P}] + k_1k_2k_{12}[\mathrm{P}]^2}{1 + (k_1 + k_2)[\mathrm{P}] + k_1k_2k_{12}[\mathrm{P}]^2} \quad (2)$$

that relate the fractional occupancy of each operator half-site, $\bar{Y}_1$ and $\bar{Y}_2$, to the total protein concentration in monomer units, [P]. The terms k_1 and k_2 are the intrinsic equilibrium association constants governing binding of a repressor monomer to each of the half-sites, and k_{12} is the equilibrium constant for the cooperative interaction. In nonlinear least-squares analysis, the data were fit to obtain the most probable Gibbs free energies where $\Delta G_i = -RT \ln k_i$.

Analysis of Sedimentation Equilibrium Data. Sedimentation data were analyzed using a version of the NONLIN program (*27*, *28*) adapted for analysis of sedimentation equilibrium data (MacNONLIN). Equilibrium sedimentation data were initially analyzed using a model for a single, homogeneous species according to the following equation (*29*):

$$c_r = \delta c + c_o \exp[M(1 - \bar{\nu}\rho)\omega^2(r^2 - r_o^2)/2RT] \quad (3)$$

where c_r is the total protein concentration at a given radial position, c_o is the protein concentration, in this case apoBirA, BirA·biotin, or BirA·bio-5′-AMP, at a reference position which is the first point in the data set, M is the molecular mass of the protein, $\bar{\nu}$ is the partial specific volume of the protein which was determined as described by Eisenstein and Beckett (*8*) to be 0.755 mL/mg, ρ is the solvent density, ω is the angular velocity of the rotor, r is the radial position in centimeters from the center of rotation, r_o is the distance in centimeters from the center of rotation for the reference position (the first point in the data set), R is the gas constant, T is the absolute temperature, and δc is a correction term for a non-zero baseline. In nonlinear least-squares analysis using a single-species model, the data were fit to the reduced buoyant molecular mass, σ, defined by

$$\sigma = \frac{M(1 - \bar{\nu}\rho)\omega^2}{RT} \quad (4)$$

where the terms are as indicated above.

Equilibrium sedimentation data for all BirA species were also analyzed using a monomer−dimer model:

$$c_r = \delta c + c_{o1}e^{\sigma}\xi + (c_{o1}{}^2K_{a1\leftrightarrow 2}e^{2\sigma_1\xi}) \quad (5)$$

where c_{o1} is the monomer concentration at some reference position, $K_{a1\leftrightarrow 2}$ is the equilibrium association constant

governing assembly of the monomer and dimer, and ξ is equivalent to $(r^2 - r_o^2)/2$, where r_o is the reference position and r is the radial position. In the analysis, the reduced buoyant molecular mass of a dimer was assumed to be twice the value for the monomer. In all data analysis, individual and global analysis of data sets obtained from samples prepared at multiple loading concentrations and run at multiple speeds were performed. The quality of the fits was assessed from the examination of the square root of the variance and the distribution of the residuals. Given the relatively low salt concentration (50 mM) present in the buffer utilized for sedimentation measurements, it is possible that nonideality resulting from charge−charge repulsion between proteins would be observed. However, in such cases one would expect to obtain nonrandom residuals as well as a decrease in the apparent molecular mass of the protein with increasing loading concentration, neither of which was observed (*30*).

RESULTS

DNaseI Footprinting. The quantitative DNaseI footprinting technique was used to assess the binding of the three BirA species to bioO. Eisenberg et al. previously showed using filter binding that biotin can activate the DNA binding function of BirA, albeit more weakly than does bio-5′-AMP (*15*). However, these results were not quantitative. While the standard buffer utilized for assessment of the holoBirA·bioO interaction in this laboratory contains 200 mM KCl, the weak affinity of apoBirA and BirA·biotin for bioO necessitated assessment of DNA binding in buffer containing a relatively low KCl (50 mM) concentration. For bioO binding measurements performed at a low salt concentration, it is important to demonstrate that the weaker binding species, in this case, apoBirA and BirA·biotin, indeed bind specifically to the operator rather than via a nonspecific mechanism. An image of a footprinting gel obtained from titration of bioO with apoBirA is shown in Figure 2. The footprint shows altered cleavage in only the region known to correspond to the bioO sequence (*16*). Moreover, this footprint is qualitatively identical to those obtained from titrations of bioO with BirA·biotin or BirA·bio-5′-AMP (data not shown). The patterns of enhancement of and protection from DNaseI digestion were identical for all three protein species. Thus, even at the low salt concentration, binding of all three BirA species to bioO is specific.

Individual site isotherms obtained from quantitation of footprint titrations of bioO with the three BirA species are shown in Figure 3. For all protein species, the two bioO half-sites titrate simultaneously with increasing protein concentrations. Moreover, on the basis of the narrow protein concentration range of approximately 1 log unit required for each titration, all species bind cooperatively to bioO. The data were subjected to nonlinear least-squares analysis using the two-individual site binding equations presented in Materials and Methods. In the analysis, the cooperative free energy was fixed at −2 kcal/mol and the best-fit values of the two intrinsic free energy terms, ΔG_1 and ΔG_2, were obtained. Results of the analyses, which are shown in Table 1, indicate that while the apoBirA species binds with the lowest affinity, the biotin species is intermediate and holoBirA binds with the highest affinity. Comparison of the total Gibbs free energies of binding indicates that biotin binding to apoBirA enhances the total binding free energy by approximately −1.6 kcal/mol. The physiological corepressor, bio-5′-AMP, effects an enhancement in bioO binding affinity of approximately −4.5 kcal/mol.

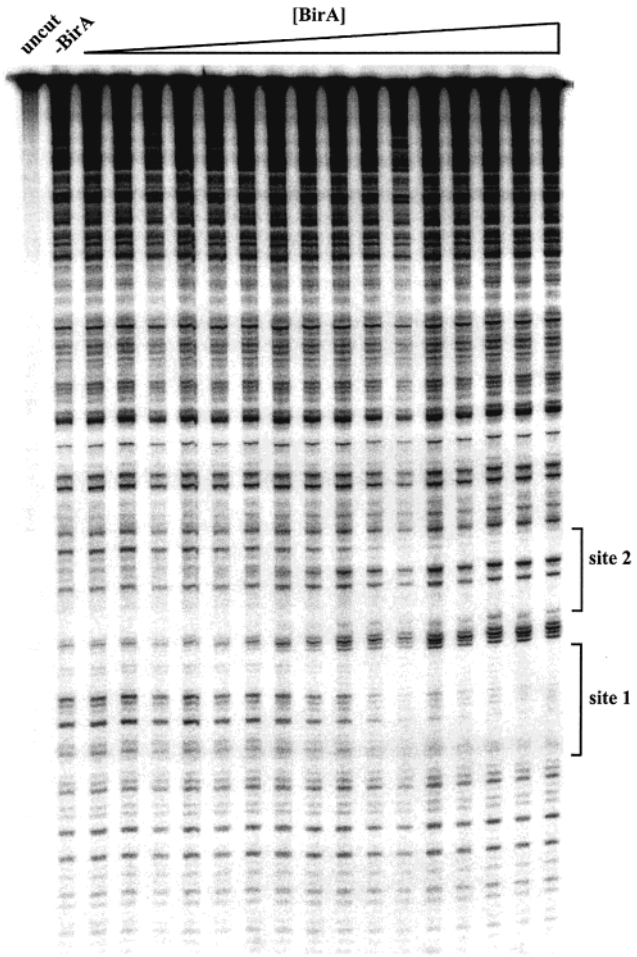

FIGURE 2: Image of a DNaseI footprint titration of bioO with apoBirA. The bioO half-sites are arbitrarily designated 1 and 2. The footprint was created in buffer containing 10 mM Tris-HCl (pH 7.50 ± 0.02 at 20 °C), 50 mM KCl, 2.5 mM $MgCl_2$, 1 mM $CaCl_2$, 20 μg/mL sonicated calf thymus DNA, and 100 μg/mL BSA.

Sedimentation Equilibrium. The assembly properties of the three BirA species were determined by sedimentation equilibrium. Data previously obtained for the three species indicated that while holoBirA dimerizes at a concentration near 10 μM, neither the biotin-bound species nor apoBirA exhibited any tendency to oligomerize (*8*). These previous measurements were, however, taken in buffer containing 200 mM KCl using relatively low protein concentrations. In this work, assembly studies of the three BirA species were performed in the low-salt buffer.

Results of the initial measurements performed on holoBirA indicated that dimerization of the protein was considerably tighter than had previously been seen in 200 mM KCl (*8*). Consequently, measurements of the assembly process required use of loading concentrations of protein as low as 2−3 μM. Results of these measurements are shown in Figure 4. Global analysis of the data using a single-species model revealed a molecular mass considerably higher than that of the protein monomer, a result consistent with self-association of the protein (Table 2). Additionally, reversible association

Table 1: DNaseI Footprinting Measurements of BioO Binding by the Three BirA Species[a]

species	ΔG_{12}[b] (kcal/mol)	ΔG_1 (kcal/mol)	ΔG_2 (kcal/mol)	(var)$^{1/2}$ [c]	ΔG_{tot} (kcal/mol)
apoBirA	−2	−8.3 ± 0.5	−7.9 ± 0.5	0.048	−18.2 ± 0.7
BirA·biotin	−2	−9.0 ± 0.3	−8.8 ± 0.3	0.026	−19.8 ± 0.4
BirA·bio-5′-AMP	−2	−10.5 ± 0.3	−10.2 ± 0.4	0.040	−22.7 ± 0.5

[a] All measurements were performed in 10 mM Tris-HCl (pH 7.50 ± 0.02 at 20 °C), 50 mM KCl, 2.5 mM $MgCl_2$, 1.0 mM $CaCl_2$, 100 μg/mL BSA, and 20 μg/mL sonicated calf thymus DNA. [b] In nonlinear least-squares analysis, the cooperative free energy was fixed at −2 kcal/mol. Uncertainties in parameters represent the 65% confidence intervals. [c] The square root of the variance of the fit.

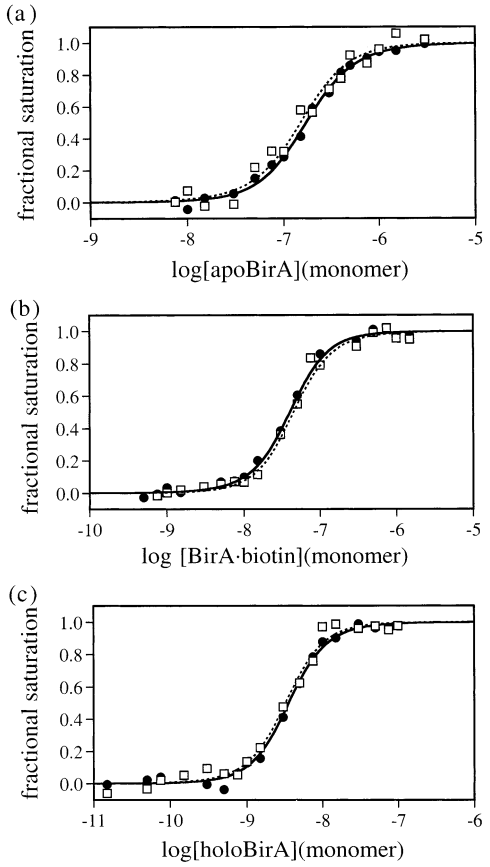

FIGURE 3: Individual site isotherms for binding of (a) apoBirA, (b) BirA·biotin, and (c) BirA·bio-5′-AMP (holoBirA) to bioO. Isotherms were obtained from DNaseI footprints quantitated as described in refs *14* and *20*: half-site 1 (□) half-site 2 (●). The solid and dashed lines are individual site isotherms generated from the best fit parameters obtained from analysis of the data for sites 1 and 2, respectively.

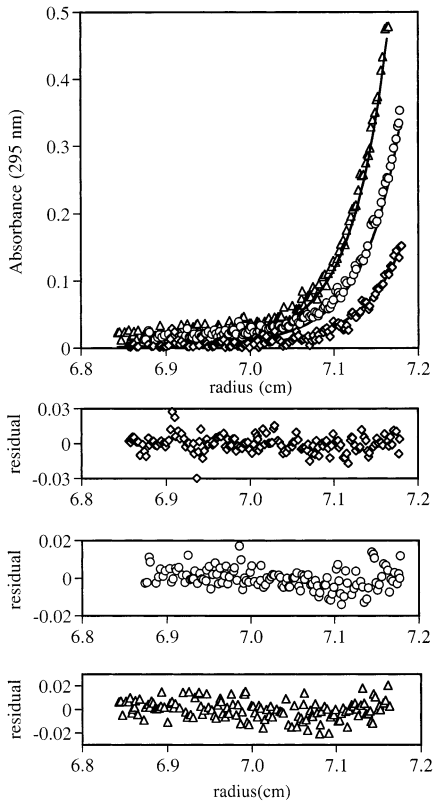

FIGURE 4: Results of sedimentation equilibrium measurements performed on BirA·bio-5′-AMP. The data obtained at loading concentrations of 2.5 (◇), 5.0 (○), and 7.5 μM (△) centrifuged at 22 000 rpm are shown. Best-fit curves obtained from global analysis of six data sets to a monomer−dimer model are shown as solid lines. The residuals in A_{295} units associated with each data set are shown below the curves.

was supported by results of analysis of individual data sets with a single-species model, which indicated an increase in the apparent molecular mass of the complex with increasing loading concentrations (data not shown). Results of analysis of the data using a monomer−dimer model (Table 2) indicate that the K_D for dimerization is approximately 1 μM. Thus, in the low-salt buffer, the dimerization is approximately 1 kcal more favorable than it is in 200 mM KCl. The broad confidence limits on the resolved dimerization free energy can be attributed to the tight dimerization, which renders the protein, even at the lowest loading concentrations that were employed, predominantly dimeric. At the lowest loading concentrations utilized for the measurements, the protein is approximately 75% dimer. The limitation of the absorption optics used to detect the protein precluded measurements at concentrations at which a major fraction of the BirA·bio-5′-AMP complex is monomeric.

Results of previous assessments of assembly of apoBirA and BirA·biotin in standard high-salt buffer indicated that neither species exhibited any tendency to dimerize (*8*). Results of initial measurements made in the low-salt buffer revealed that the two species dimerize weakly. To assess the assembly properties of these two species, protein concentrations of up to 0.10 mM were employed. Given these high concentrations, measurements were performed using the 3 mm path length cells and scans were obtained on the red edge of the absorption spectrum of the protein at 300 nm. Results of representative measurements performed on the biotin-bound species are shown in Figure 5, and global analysis of the data provides convincing evidence that the system is described well by a monomer−dimer model. First, analysis of the data using a single-species model yielded an apparent molecular mass that was higher than that of the protein monomer (Table 2). Moreover, analysis of individual data sets using this model indicated increasing apparent molecular mass with increasing loading concentration.

Table 2: Sedimentation Equilibrium Measurements of the Assembly Properties of the Three BirA Species

species[a]	single-species MW[b] (Da)	monomer−dimer[b] K_D (M)	$\Delta G°_{DIM}$ (kcal/mol)[c]	(var)$^{1/2}$ [d]
apoBirA	37 683 (36 552−39 000)			0.0054
		1.4 (1.0−2.0) × 10^{-3}	−3.8 (−3.6 to −4.0)	0.0050
BirA·biotin	40 687 (39 490−41 644)			0.0056
		0.9 (0.7−1.2) × 10^{-3}	−4.1 (−4.3 to −3.9)	0.0049
BirA·bio-5′-AMP	57 469 (54 454−60 672)			0.0072
		1.5 (0.8−2.7) × 10^{-6}	−7.8 (−7.5 to −8.2)	0.0071

[a] All measurements were performed in 10 mM Tris-HCl (pH 7.50 ± 0.02 at 20 °C), 50 mM KCl, and 2.5 mM $MgCl_2$. Sufficient ligand to fully saturate the protein was present in the samples containing complexes. [b] Resolved molecular masses and equilibrium dimerization constants were obtained from global analysis of data obtained at multiple rotor speeds and loading concentrations. Loading concentrations for apoBirA were 50 and 100 μM, and rotor speeds were 22 000, 24 000, and 26 000 rpm. Loading concentrations for BirA·biotin were 40 and 90 μM, and rotor speeds were 20 000, 22 000, and 24 000 rpm. Loading concentrations for the BirA·bio-5′-AMP complex were 2.5, 5.0, and 7.5 μM, and rotor speeds were 22 000 and 24 000 rpm. The values in parentheses provide the 65% confidence intervals. The reduced molecular mass of the monomer was fixed at a value obtained from sedimentation equilibrium measurements performed on apoBirA at a low (2.5 μM) loading concentration. [c] Gibbs free energies were calculated from the equilibrium dissociation constants using the relationship $\Delta G_{DIM} = RT \ln K_{DIM}$. [d] Square root of the variance.

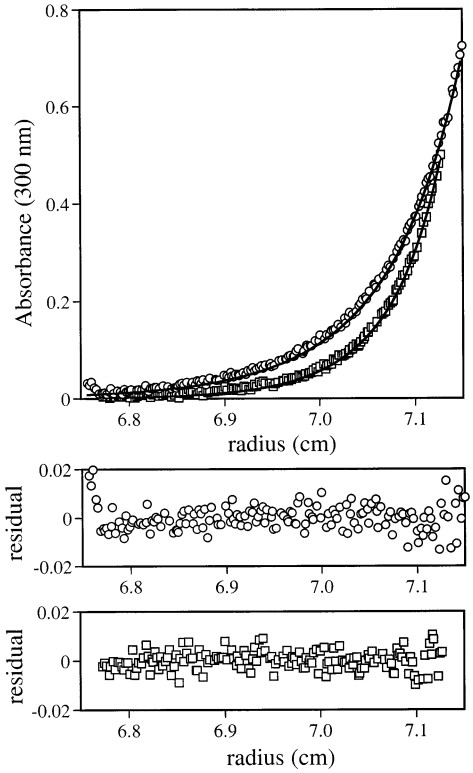

FIGURE 5: Results of sedimentation equilibrium measurements performed on BirA·biotin. Data were obtained from data sets for samples prepared at a loading concentration of 90 μM and run at speeds of 20 000 (○) and 24 000 (□) rpm. The best-fit curves shown with the data were obtained from global analysis of six data sets obtained from samples prepared at 40 and 90 μM and centrifuged at 20 000, 22 000, and 26 000 rpm. Residuals of the fits in A_{300} units for the two curves are shown in the bottom panels.

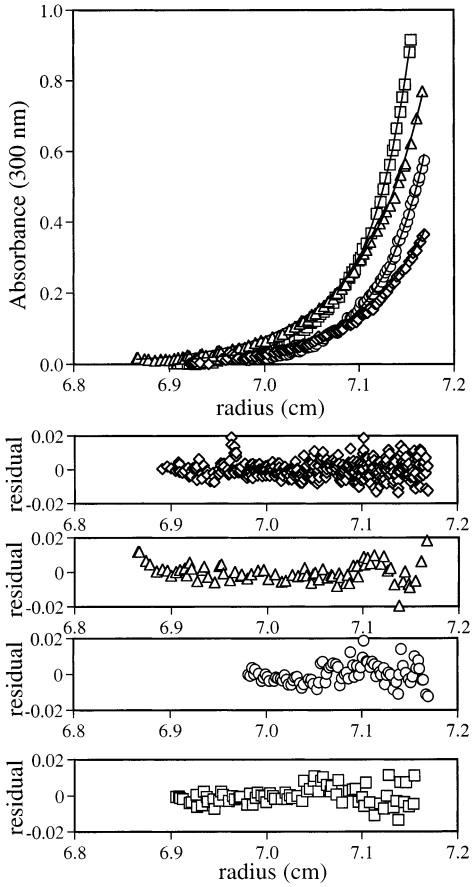

FIGURE 6: Sedimentation equilibrium measurements performed on apoBirA. The loading concentrations were 50 (◇ and ○) and 100 μM (△ and □), and the samples were centrifuged at 22 000 and 26 000 rpm, respectively. The lines were obtained from global fits of six data sets to a monomer−dimer model. Residual plots in A_{300} units are shown for the data sets included in the figure.

Second, as indicated by the magnitude of the square root of the variance of the fits, the data are better described by the monomer−dimer than the single-species model. The equilibrium dissociation constant obtained from the data analysis is approximately 1 mM, and the confidence intervals are tight. Given this weak dimerization process, at the highest concentration of the complex the fraction of the protein that is dimer is approximately 25%. However, since the end point of the assembly process is well-established by structural and thermodynamic data to be the dimer, analysis of the data using the monomer−dimer model is appropriate.

Results of sedimentation measurements performed on the apoBirA species are shown in Figure 6. Global analysis of the data using a single-species model yielded a molecular mass significantly higher than the value of 35 313 Da expected for the monomeric protein (Table 2). Analysis of the data using a monomer−dimer model revealed an equilibrium dimerization constant of 1−2 mM. This value may represent a lower limit for the equilibrium dissociation constant since the quality of the fit, as judged by the square root of the variance, is only marginally better for the monomer−dimer model than for the single-species model. However, a value of 1−2 mM was reproducibly obtained, and the confidence intervals are narrow.

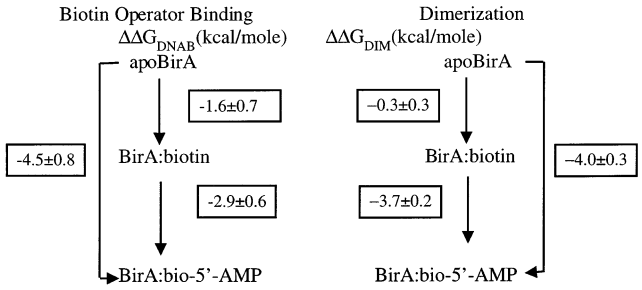

FIGURE 7: Summary of measurements of the energetics of dimerization and bioO binding properties for the three BirA species. The differences in the total Gibbs free energies of bioO binding ($\Delta\Delta G_{DNAB}$) for pairs of species are shown on the left. The same quantities for dimerization energetics ($\Delta\Delta G_{DIM}$) are shown on the right.

DISCUSSION

The proposed mechanism of allosteric activation of BirA is that the corepressor, bio-5′-AMP, enhances the occupancy of bioO by increasing the stability of the repressor homodimer interface. Support for this mechanism is provided by results of combined thermodynamic and structural measurements (*8*−*10*). The experiments presented in this work are designed to directly test this model. If allostery in this system is transmitted solely through the BirA homodimer interface, it is expected that for any two of the three BirA species examined, apoBirA, BirA·biotin, and BirA·bio-5′-AMP, the measured difference in the bioO binding energetics should be equivalent to measured differences in the dimerization energetics. A summary of the results is shown in Figure 7. First, the results are consistent with the idea that the affinities of the three species for bioO track with the stabilities of the dimers formed by the three species. The more stable the homodimer formed by a species, the greater its affinity for bioO. Moreover, the data obtained for the apoBirA/holoBirA pair indicate that the enhancement in bioO binding energetics that accompanies bio-5′-AMP binding is identical to the additional free energy of dimerization. This supports the simple notion that the allosteric mechanism associated with bio-5′-AMP binding to BirA is mediated solely through the monomer−monomer interface.

The results obtained for any pair of BirA species that includes the biotin-bound repressor deviate from a mechanism in which allostery is transmitted solely through the monomer−monomer interface of the BirA dimer. First, it is instructive to analyze the results obtained with the biotin- and bio-5′-AMP-bound BirA. While the difference in the total Gibbs free energy of bioO binding for these two species is approximately −2.9 kcal/mol, the gap in the dimerization energetics is approximately −3.7 kcal/mol. Thus, the enhancement in dimerization energetics resulting from replacing biotin with bio-5′-AMP is significantly greater than the enhancement in bioO binding. Discrepancies are also found in the differences in assembly and bioO binding energetics for the apoBirA and BirA·biotin species. The enhancement in bioO binding associated with switching the repressor from the apo to the biotin-bound form is approximately −1.6 kcal/mol. However, if it is assumed that the upper limit of 1−2 mM obtained for the equilibrium dimerization constant of the aporepressor is accurate, the difference in the dimerization energetics of the two species of -0.3 ± 0.3 is insignificant. Therefore, for this pair, the enhancement in dimerization energetics is marginal to nonexistent while the enhancement in bioO binding energetics is large.

The nearly perfect correlation between the enhancement in dimerization and bioO binding energetics observed for the apo-BirA and bio-5′-AMP-bound species is consistent with the structural interpretation that allostery in the biotin repressor is mediated solely through the dimerization interface. While this is the most straightforward interpretation of the data, it is based on the assumption that the enhanced assembly energetics associated with bio-5′-AMP binding are transmitted with 100% efficiency to the DNA binding process. However, additional support for this simple interpretation is derived from results of measurements of the assembly and bioO binding energetics of BirA mutants (*9*) as well as the results of structural studies described in the introductory section. The results obtained with the biotin-bound species deviate from this simple model and indicate that dimerization and DNA binding can be uncoupled for the repressor/substrate pair. These results are, moreover, consistent with the notion that for biotin the allosteric effect occurs at the level of DNA binding by enhancing the affinity of the repressor monomer for an operator half-site. In principle, this possibility could be directly investigated by assessing binding of the different liganded forms of the BirA monomer to a bioO half-site. However, despite several attempts (*31*), the tight coupling of dimerization and DNA binding in the system has prevented the success of such measurements. The observation that the allosteric response may be mediated at the level of DNA binding suggests the involvement of structural regions in BirA in addition to the dimerization interface in transmission of the allosteric response. Results of previous experiments provide evidence that a domain−domain interface between the DNA binding and central domains of the protein may be important in the allosteric mechanism. First, a truncated mutant of BirA in which the N-terminal DNA binding domain was deleted has been subjected to functional analysis (*32*). Results of these measurements indicated that in addition to its inability to bind bioO the truncated mutant bound biotin and bio-5′-AMP with an affinity significantly lower than that of the intact protein. This suggests communication takes place between these two domains. In addition, results of chemical and enzymatic probing of BirA in the absence and presence of ligands indicate that the flexible loop consisting of residues 212−233 becomes protected from proteolytic and chemical cleavage concomitant with small ligand binding (*25*, *33*). The extent of protection is greater for adenylate than for biotin binding. Evaluation of these results in the context of the known structure of the biotin-bound repressor (Figure 1) has led to the prediction that in the adenylate-bound structure a closer association of the N-terminal and DNA binding domains will be observed and that this interaction may involve residues 212−233.

The results of sedimentation equilibrium measurements performed on the biotin and adenylate-bound repressor indicate that a relatively small structural change in a regulatory ligand can have profound consequences for the thermodynamics of assembly of a protein. The dimerization of the biotin-bound repressor is very weak and in low salt is characterized by an equilibrium constant in the millimolar concentration range. The bio-5′-AMP-bound protein dimerizes with an equilibrium constant that is 1000-fold tighter.

Structural studies suggested that the enhanced dimerization associated with biotin binding is provided by the disorder to order transition that accompanies binding of the ligand to BirA. This preordering of the loops lowers the entropic penalty to dimerization. Although this conclusion may, in part, explain the more stable dimerization of the adenylate-bound protein, the available structural data provide no information about the origin of the −3.7 kcal/mol enhancement in dimerization resulting from addition of the AMP moiety to the biotin ligand. However, this large energetic difference is suggestive of significant structural differences between the adenylate- and biotin-bound BirA dimer.

Given the significantly greater stability of the bio-5′-AMP-bound BirA dimer compared to the BirA·biotin dimer, it is tempting to question the relevance of the structure of the latter species for understanding the structure of the physiologically relevant dimer. However, results of thermodynamic studies of mutants in the surface loops located in the known BirA·biotin dimer interface support the idea that it does indeed provide information about the BirA·bio-5′-AMP dimer. Mutations in these loops have been shown to result in large energetic penalties for both bioO binding and dimerization (*9*). Moreover, these measurements were all performed on the bio-5′-AMP-bound species of the mutants. These same mutations have been shown to prevent repression of transcription initiation at the biotin operon control region in vivo. Thus, essential features of the adenylate-bound dimer are provided in the structure of the biotin-bound species.

A considerable electrostatic component appears to be associated with dimerization of BirA. While the equilibrium dimerization constant previously measured in standard buffer containing 200 mM KCl is approximately 10 μM, the value obtained in 50 mM KCl is 1 μM. Thus, decreasing the KCl concentration from 200 to 50 mM renders the dimerization process more favorable by −1 kcal/mol. Examination of the structure of the BirA·biotin dimerization structure reveals at least one source of this electrostatic component. Residues D197 and R119, which are both found in disordered loops in the aporepressor structure, are in close juxtaposition in the dimer structure. Mutation of either residue results in decreased bioO binding affinity as well as a decrease in the ability of the protein to dimerize (*9*). Two dyad symmetric salt bridges are formed between these two residues in each dimer. Thus, these two interactions constitute a portion of the electrostatic component of the dimerization energetics. Determination of the magnitude of the electrostatic component of the dimerization energetics will require a more systematic investigation of the dependence of the dimerization process on salt concentration.

A number of biological processes are regulated via controlled protein association. Among these are the transcription initiation regulatory systems in which the occupancy of a target DNA sequence by a transcriptional activator or repressor is subject to control. Processes that regulate the assembly reaction include small ligand binding, post-translational modification, and other protein−protein interactions. While these regulatory processes are appreciated at a phenomenological level, it is not clear if the functional energetics of the systems reflect only control at the level of protein−protein association. The studies of the biotin repressor presented in this work indicate that although the protein assembly reactions are responsible in large part for the enhancement of DNA binding energetics resulting from corepressor binding additional regions of the protein structure may be involved in transmission of the allosteric response.

REFERENCES

1. Bailey, M. F., Davidson, B. E., Minton, A. P., Sawyer, W. H., and Howlett, G. J. (1996) The effect of self-association on the interaction of the *Escherichia coli* regulatory protein TyrR with DNA, *J. Mol. Biol. 263*, 671−684.
2. Correia, J. J., Chacko, P. M., Lam, S. S., and Lin, K. (2001) Sedimentation studies reveal a direct role of phosphorylation in Smad3:Smad4 homo- and hetero-trimerization, *Biochemistry 40*, 1473−1482.
3. Chang, J. F., Phillips, K., Lundback, T., Gstaiger, M., Ladbury, J. E., and Luisi, B. (1999) Oct-1 POU and octamer DNA co-operate to recognise the Bob-1 transcription co-activator *via* induced folding, *J. Mol. Biol. 288*, 941−952.
4. Matthews, K. S., Falcon, C. M., and Swint-Kruse, L. (2000) Relieving repression, *Nat. Struct. Biol. 7*, 184−187.
5. Schumacher, M. A., Choi, K. Y., Lu, F., Zalkin, H., and Brennan, R. G.(1995) Mechanism of corepressor-mediated specific DNA binding by the purine repressor, *Cell 83*, 147−155.
6. Bell, C. E., and Lewis, M. (2000) A closer view of the conformation of the Lac repressor bound to operator, *Nat. Struct. Biol. 7*, 209−214.
7. Beckett, D. (2001) Regulated protein assembly in transcription initiation, *J. Mol. Biol. 314*, 335−352.
8. Eisenstein, E., and Beckett, D. (1999) Dimerization of the *Escherichia coli* biotin repressor: corepressor function in protein assembly, *Biochemistry 38*, 13077−13084.
9. Kwon, K. H., Streaker, E. D., Ruparelia, S., and Beckett, D. (2000) Multiple flexible surface loops in the biotin repressor function in corepressor-induced dimerization, *J. Mol. Biol. 305*, 821−833.
10. Weaver, L., Kwon, K. H., Beckett, D., and Matthews, B. W. (2001) Corepressor-induced organization and assembly of the biotin repressor: A model for allosteric activation of a transcriptional regulator, *Proc. Natl. Acad. Sci. U.S.A. 98*, 6045−6050.
11. Barker, D. F., and Campbell, A. M. (1981) Genetic and biochemical characterization of the *birA*gene and its product: evidence for a direct role of biotin holoenzyme synthetase in repression of the biotin operon in *Escherichia coli*, *J. Mol. Biol. 146*, 469−492.
12. Barker, D. F., and Campbell, A. M. (1981) The *birA* gene of *Escherichia coli* encodes a biotin holoenzyme synthetase, *J. Mol. Biol. 146*, 451−467.
13. Cronan, J. E., Jr. (1989) The *E. coli bio* operon: Transcriptional repression by an essential protein modification enzyme, *Cell 58*, 427−429.
14. Lane, M. D., Rominger, K. L., Young, D. L., and Lynen, F. (1964) The enzymatic synthesis of holotranscarboxylase from apotranscarboxylase and (+) biotin: II. Investigation of the reaction mechanism, *J. Biol. Chem. 239*, 2865−2871.
15. Prakash, O., and Eisenberg, M. A. (1979) Biotinyl 5′-adenylate: Corepressor role in the regulation of the biotin genes of *Escherichia coli* K-12, *Proc. Natl. Acad. Sci. U.S.A. 76*, 5592−5595.
16. Abbott, J., and Beckett, D. (1993) Cooperative binding of the repressor of biotin biosynthesis to the biotin operator, *Biochemistry 32*, 9649−9656.
17. Wilson, K. P., Shewchuk, L. M., Brennan, R. G., Otsuka, A. J., and Matthews, B. W. (1992) The *E. coli* biotin holoenzyme synthetase/*bio* repressor crystal structure delineates the biotin and DNA-binding domains, *Proc. Natl. Acad. Sci. U.S.A. 89*, 9257−9261.
18. Chapman-Smith, A., Mulhern, T. D., Whelan, F., Cronan, J. E., Jr., and Wallace, J. C. (2001) The C-terminal domain of biotin protein ligase from *E. coli* is required for catalytic activity, *Protein Sci. 10*, 2608−2617.
19. Weaver, L., Kwon, K. H., Beckett, D., and Matthews, B. W. (2001) Competing protein:protein interactions are proposed to control the biological switch of the *E. coli* biotin repressor, *Protein Sci. 10*, 2618−2622.
20. Koradi, R., Billeter, M., and Wüthrich, K. (1996) MOLMOL: A program for display and analysis of macromolecular structures, *J. Mol. Graphics 14*, 51−55.
21. Kwon, K. H., and Beckett, D. (2000) Function of a conserved sequence motif in biotin holoenzyme synthetases, *Protein Sci. 9*, 1530−1539.

22. Brenowitz, M., Senear, D. F., Shea, M. A., and Ackers, G. K. (1986) Quantitative DNaseI footprint titration: A method for studying protein-DNA interactions, *Methods Enzymol. 130*, 133−181.
23. Maniatis, T., Fritsch, E. F., and Sambrook, J. (1982) *Molecular Cloning, A Laboratory Manual*, Cold Spring Harbor Laboratory Press, Plainview, NY.
24. Xu, Y., and Beckett, D., (1994) Kinetics of biotinoyl-5′-adenylate synthesis catalyzed by the *E. coli* repressor of biotin biosynthesis and the stability of the enzyme−product complex, *Biochemistry 33*, 7354−7360.
25. Xu, Y., Nenortas, E., and Beckett, D. (1995) Evidence for distinct ligand-bound conformational states of the multifunctional *Escherichia coli* repressor of biotin biosynthesis, *Biochemistry 34*, 16624−16631.
26. Roark, D. E. (1976) Sedimentation equilibrium techniques: Multiple speed analyses and an overspeed procedure, *Biophys. Chem. 5*, 185−196.
27. Johnson, M. L., and Faunt, L. M. (1992) Parameter estimation by least-squares methods, *Methods Enzymol. 210*, 1−37.
28. Johnson, M. L., Correia, J. J., Yphantis, D. A., and Halvorson, H. R. (1981) Analysis of data from the analytical ultracentrifuge by nonlinear least-squares techniques, *Biophys. J. 36*, 575−588.
29. Laue, T. M. (1995) Sedimentation equilibrium as a thermodynamic tool, *Methods Enzymol. 259*, 427−452.
30. Laue, T. M., Shah, B. D., Ridgeway, T. M., and Pelletier, S. L. (1992) Computer-aided interpretation of analytical sedimentation data for proteins, in *Analytical Ultracentrifugation in Biochemistry and Polymer Science* (Harding, S. E., Rowe, A. J., and Horton, J. C., Eds.) pp 90−125, Royal Society of Chemistry, Cambridge, U.K.
31. Streaker, E. D., and Beckett, D. (1998) Coupling of site-specific DNA binding to protein dimerization in assembly of the biotin repressor-biotin operator complex, *Biochemistry 37*, 3210−3219.
32. Xu, Y., and Beckett, D. (1996) Evidence for inter-domain interaction in the *Escherichia coli* repressor of biotin biosynthesis from studies of an N-terminal domain deletion mutant, *Biochemistry 35*, 1783−1792.
33. Streaker, E. D., and Beckett, D. (1999) Ligand-linked structural changes in the *Escherichia coli* biotin repressor. The significance of surface loops for binding and allostery, *J. Mol. Biol. 292*, 619−632.

BI0203839